THE PROPAGATION CHARACTERISTICS OF LASER-GENERATED GUIDED WAVE IN CARBON STEEL PLATE WITH WALL-THINNING

Jong-Ho Park[1], Joon-Hyun Lee[1], Min-Rae Lee[2]

[1]School of Mechanical Engineering, Pusan National University, San 30 Jangjeon-dong, Kumjeong-gu, Busan, 609-735, Korea
[2]Research Center for Failure Analysis and Reliability, Pusan National University, San 30 Jangjeon-dong, Kumjeong-gu, Busan, 609-735, Korea

Abstract

The objective of this study is to evaluate carbon steel plate with wall-thinning by using guided waves. To accomplish this purpose, the plates with various types of defects were used as testing specimens. In addition, a Nd:YAG pulse laser and an air-coupled transducer were applied to the generation and the detection of guided waves. The specimens were divided into two groups according to factors, such as the width and the depth of thinned area. In first group, all thinned depths of defects were 1mm and their width was 20mm, 40mm and 60mm respectively. The other group was that all defects were 20mm in width and each of thickness reduction was 0.5mm, 1.0mm and 1.5mm. The result is that guided wave modes, such as A0 and S0 mode, passed each of defect change regularly in accordance with the variation of the depth and width of wall-thinning in their group velocities and frequencies. This fact shows that the above-mentioned characteristics of guided waves can be used as the tool for the evaluation of wall thinning.

1. Introduction

Ultrasound has been used in the fields of nondestructive testing (NDT) and evaluation (NDE) for many decades. However, although various ultrasonic techniques have been studied, the conventional transducers such as PZT sensor have been mainly used to generate and detect ultrasound until recently. Such transducers are unsuitable for NDT or NDE in some areas of industrial plant, automatic manufacturing system and high temperature environments due to their contacting nature and general requirement for a coupling medium [1-2]. These limited applications of ultrasound arouse the need of new techniques to overcome this problem and utilize ultrasound more efficiently than conventional ones, and one of the most unique of these is non-contact ultrasound. Non-contact techniques permit generation and detection of acoustic waves with less modification of the detected waveform or frequency spectrum [3]. In addition, they can make measurements in hot and cold materials and in other hostile environments, in geometrically difficult to reach locations and at relatively large distances from the test structure. These non-contact acoustical techniques include air-coupling, electromagnetic acoustic transducers (EMATs), laser generation and optical holographic detection. Among these, laser based ultrasonic method is a emerging powerful tool in the field of non-destructive evaluation due to the ability to operate remote from the sample surface, on-line process control and rapid inspection of various structures [4-6]. Such laser ultrasonics is a well known method to create ultrasound of extremely broad bandwidth in solids. When laser beam is illuminated in a solid, many types of waves are generated and particularly the intensity of the laser beam controls the type of generated mechanism [7]. Two different mechanisms generated by the impact of pulsed laser beams on a solid are ablation and thermoelasticity as shown in Figures 1(a)-(b). Thermoelastic regime in Figure 1(a) is truly non-destructive in the sense that it consists of absorption of a laser pulse possessing moderate energy in a finite depth of the material such that thermal expansion causes a volume change and consequently an elastic wave. In the ablation range, on the other hand, a laser pulse with the much high power density level causes the formation of plasma and rapid evaporation of materials from the surface as shown in Figure 1(b). Although the surface of the test object is slightly damaged when ablation occurs, in certain cases the amount of damage is acceptable when such a generation process is the only way to generate ultrasonic waves of sufficient amplitude in a non-contact manner [8]. The interesting fact of these mechanisms is that a certain type of elastic waves which provide a means of material characterization and detect identification is generated. This study is focused on guided waves that are well-known lamb waves among various elastic waves. Generally, guided waves contain the

information of inspection object with one-point inspection technique using them can evaluate thickness degradation for large-area structures such as pipes and vessels quickly [9-10]. In addition, it can realize reliable inspection for objects with limited access. The aim of this study is the development of the non-contact technique which can detect and evaluate various types of defects in plate examination, and therefore the using this feature of guided waves. Non-contact system used for this purpose consisted of laser generation of guided waves and an air-coupled transducer was used since this non-contact transducer combination [11-12] can be used at a much greater distance from the sample and can make the system flexible according to the inspected object.

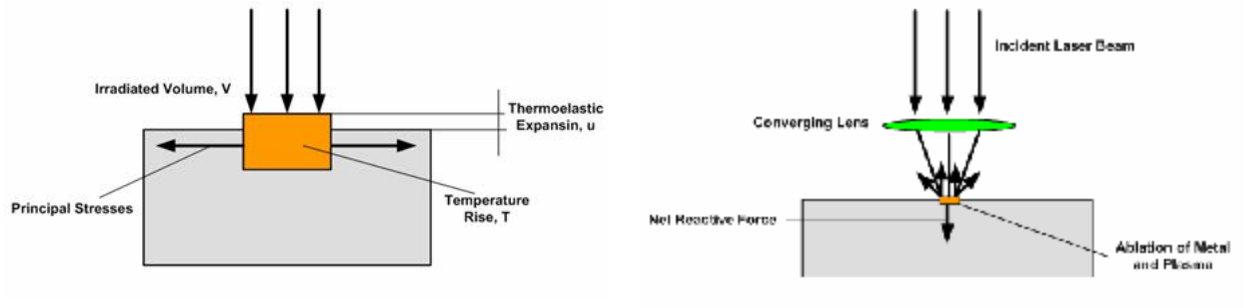

(a) thermoelastic regime (b) ablation regime

Figure 1: *Schematic diagram of mechanism induced by the incident of laser pulse on a sample surface.*

2. Determination of Linear Slit array

In nondestructive testing, laser ultrasonic methods have some drawbacks when compared to more conventional contact transducer techniques with regard to generation efficiency and detection sensitivity [13]. Hence, several researchers have developed techniques that can improve the sensitivity of inspection and the directivity of laser-generated guided waves. Linear slit array is also one of the alternative methods and has the advantages of increment on directivity of laser-generated ultrasound and improvement in S/N ratio as well as the optional generation of guided wave mode. In this study, linear slit array is used as the tool to generate desired modes, and therefore it is important to design the suitable slit. It is known that the maximum magnitude of generated wave corresponds to the element width equal to 50% of slit spacing. In addition, S/N ratio of generated mode is improved according to the increment of the number of elements [14-15]. This fact is demonstrated in this study as shown in Figure 2. Figures 2(a)-(d) represent the magnitude of the signals received by air-coupled transducer when element width varies for 4.5mm-slit spacing which is element size plus gap between slit elements.

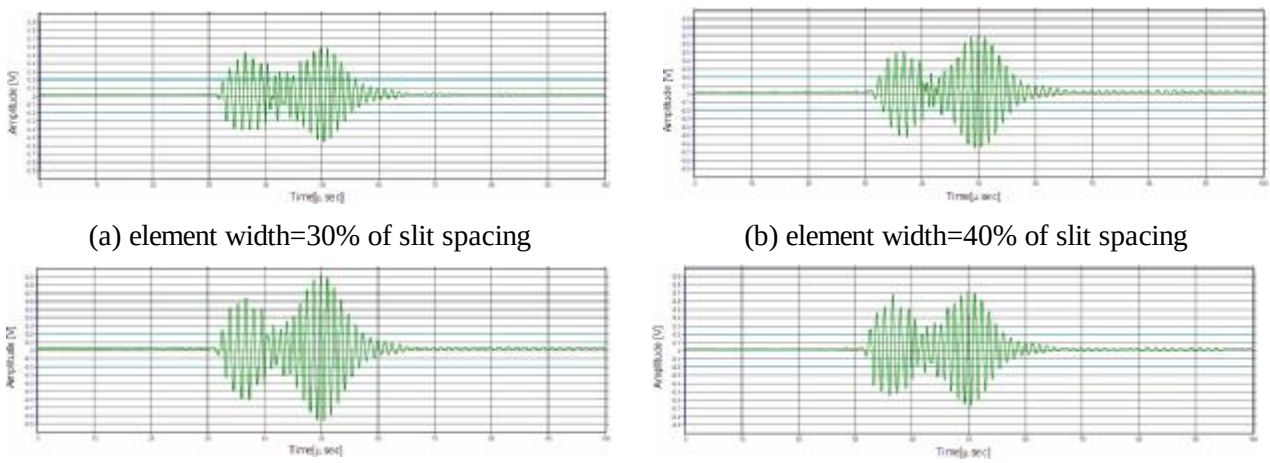

(a) element width=30% of slit spacing (b) element width=40% of slit spacing

(c) element width=50% of slit spacing (d) element width=60% of slit spacing

Figure 2: *RF signal generated in 4mm thick pipe according to width of element using 4.5mm-wavelength.*

The result presented in Figure 3 shows that the amplitude of 2.25mm slit width is the highest in all signals and then that of the signal grows low. From this result, the optimum element width of 4.5mm-slit array used in this study is determined 2.25mm.

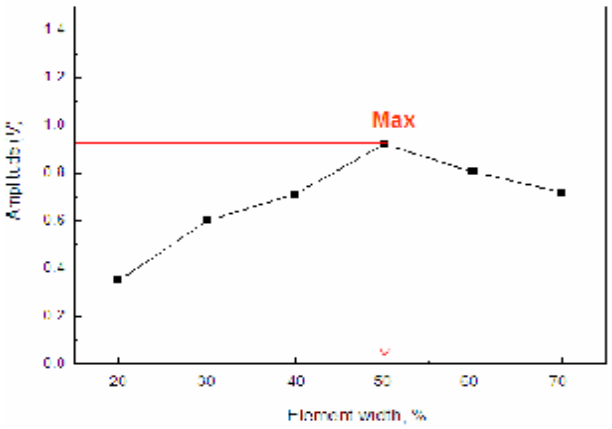

Figure 3: *The RF magnitude value versus element width.*

3. Selective Generation and Reception of Guided Waves

The problem in laser based guided wave testing is the difficulty of generating a desired mode due to the dispersive nature of Lamb waves [16]. While the excitation of a particular mode is made by a laser pulse, the different components of the wave will travel with different speeds and at least two modes are present even at low frequency range. This could make the evaluation of defect difficult due to interpretation of received signal. In this study, the selective generation and reception of guided wave modes are achieved by the technique that used the relation of dispersion curves and linear slit array [17]. Figures 4(a)-(b) show the process of selective generation using this linear slit array. The elements gap(Δs) in Figure 4(a) is equal to the wavelength of generated modes and is illustrated as the diagonal line with a slope of $\Delta s/d$ in Figure 4.

The active modes lie on at the intersection points between the line and the phase velocity dispersion curves, and therefore it possible to generate specific modes selectively by adjusting the elements gap. The method to receive the modes generated by the above-mentioned technique is to rotate the air-coupled transducer by the angle based on Snell's law for the propagation velocity in air(C_{air}) and the phase velocity of the specific mode(C_P) as shown in Equation 1. In this study, the velocity of wave in air is 340 m/s and the phase velocity of modes is obtained in Figure 4.

$$\theta = \sin^{-1}\left(\frac{C_{air}}{C_P}\right) \qquad (1)$$

This study adopted the modes of A0 and S0 as the suitable modes for experiments due to readily excited, received experimentally at low frequency-thickness and only slightly dispersive [18]. Table 1 shows frequencies, phase velocities, reception angles of A0 and S0 modes at 4.5mm slit spacing. In the process of this calculation, the velocity of wave in air was 340 m/s and the phase velocity of modes was obtained from the dispersion curves in Figure 4.

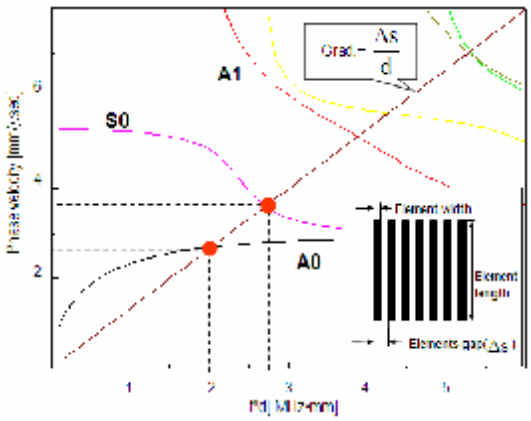

Figure 4*: Determination of desired modes using the relation between slit gap and the wavelength of generated signal in phase velocity dispersion curve.*

Table 1: Theoretical values of A0 and S0 modes at 4.5mm wavelength on 6mm-thick plate

Wavelength [mm]	Mode	Frequency[MHz]	Phase velocity[mm/μsec]	Receiving angle[θ°]
4.5	A0	0.63	3.08	6.3
	S0	0.73	3.28	5.9

4. Specimen and Experimental Setup

The tests in this study were performed to investigate the interaction between the modes, A0 and S0, and the thickness reduced defect with the different shape of its edge. In order to achieve this purpose, quadrate and elliptical defect of constant width 64mm and varying depth 1.2, 2.4 or 3.6mm respectively was machined on the carbon steel plate with 6mm thickness as shown in Figure 5. These defects are the simplest forms of the edge of defect to investigate the variation of A0 and S0 mode induced by the shape of defect. Figure 6 shows the experimental arrangement to evaluate these defects using guided waves. As shown in this figure, the hybrid system consisted of Nd:YAG pulse laser and an air-coupled transducer was applied to the generation and reception of particular modes of guided waves. In this system, the laser and air-coupled transducer are positioned on the same side of the plate and the distance between them is constant 140mm in all tests in order to evaluate only the effect of the shape of the defect on the variation of the modes excluding that of the propagating distance of A0 and S0 mode. Similarly, the stand-off between the air-coupled transducer and the outer surface of the plate is constant 15mm. In this test, the elements gap of linear slit array was determined as 4.5mm and the width of each element as 2.25mm. In addition, the element length was 20mm and the number of the elements 7 as shown in Figure 4. This configuration of the slit was designed for the optimum generation of the modes and demonstrated by several tests. By this slit, the transmitted beam act as line source on the plate and generates the waves with the wavelength corresponding to the elements gap. Here, a wavelength of Nd:YAG pulse laser was 532nm and its pulse energy was 32mJ. The waves generated by the transmitted beam propagate 140mm and are received by the air-coupled transducer with the bandwidth of 0.04 to 2.25MHz after the interaction of the defect located 40mm from the end of the slit array. Subsequently the signals received by air-coupled transducer are magnified by the amplifier and are displayed through the signal averaging scheme with 1000 sampling data on the screen of the oscilloscope. Finally, the FFT and time-frequency analysis of received signals are carried out in the computer.

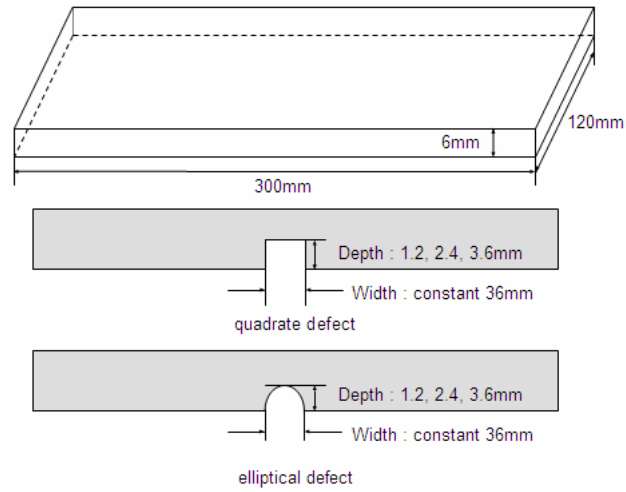

Figure 5: *Configuration of plate and defects for experiments.*

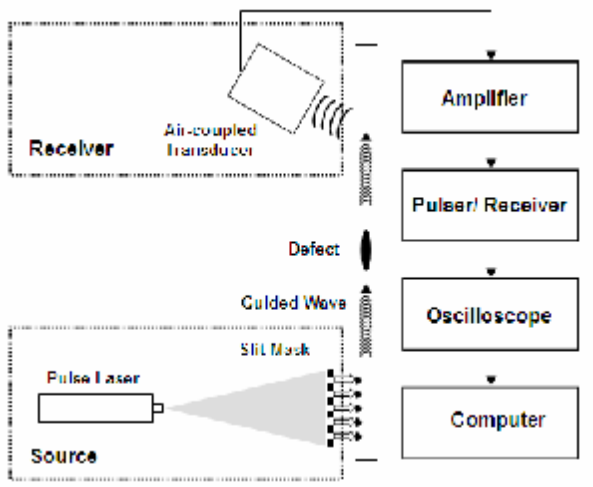

Figure 6: *schematic diagram of experimental setup for detecting defect.*

5. Experimental Results

5.1. Guided wave interaction with quadrate defects of varying depth

Figures 7(a)-(d) show the responses received by the air-coupled transducer with the angle of 6.3 degrees after interaction with no defect, 1.2, 2.4, and 3.6mm-deep quadrate defect respectively. The signals in Figures 6(a)-(d) are dominated by the A0 mode, though some evidence of S0 mode is seen, with the deeper defects. This fact indicates that the mode conversion of S0 to A0 mode is generated mainly for quadrate defect This result is demonstrated in Figures 8(a)-(d) showing the result of carrying out a time-frequency analysis on the

responses of quadrate defects with varying depth. As quency of 0.63MHz and S0 mode with that of 0.73MHz emerge concurrently at no defect, and then the magnitudes of A0 and S0 modes become smaller at 1.2mm-deep defect. However, the appearance of A0 mode is increasingly apparent again from the defect with 2.4mm depth. On the other hand, S0 mode becomes smaller continuously by its disappearance. As shown in Figure 9(a) showing the plots of magnitude of each mode and the normalized ratio of them, the magnitude of A0 mode and S0 mode decrease roughly as the defect depth increases. However, the variation is not linear, thus it is shown in these Figures, A0 mode with the fre- difficult to estimate defect depth using the magnitude of the frequency of each mode. In contrast, the ratio of the magnitude of A0 to that of S0 shows the proportional trend according to the defect depth. This result indicates that the mode conversion of S0 to A0 mode is generated regularly according to increment of quadrate defect depth and therefore it is possible to evaluate the depth of quadrate defect if the ratio of A0 and S0 mode in the signal received by the receiver after the interaction with the defect can be calculated.

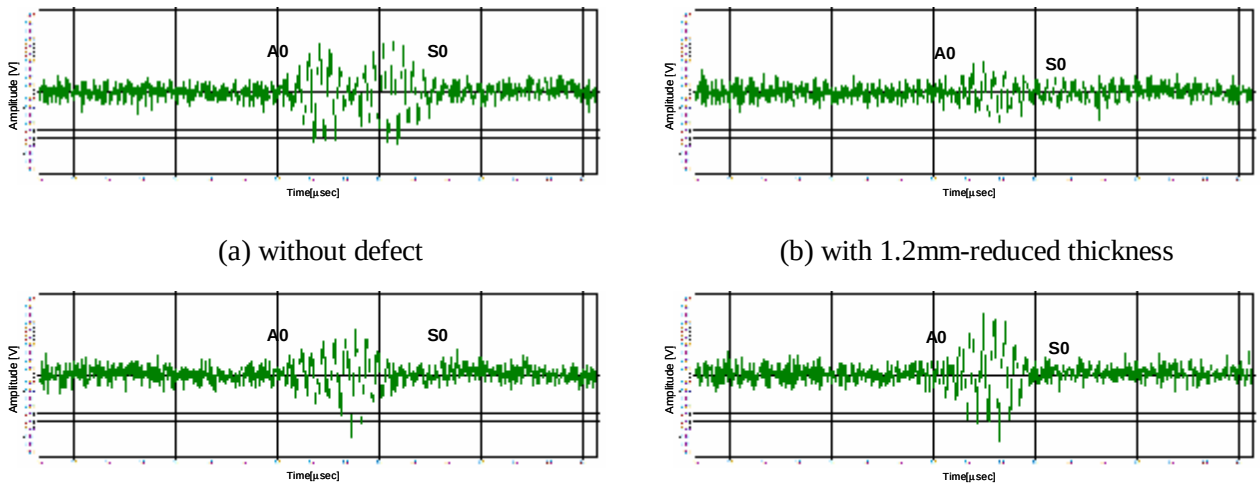

(a) without defect

(b) with 1.2mm-reduced thickness

(c) with 2.4mm-reduced thickness

(d) with 3.6mm-reduced thickness

Figure 7: *Time domain signals of quadrate defect on 6mm-thick plate according to defect depth.*

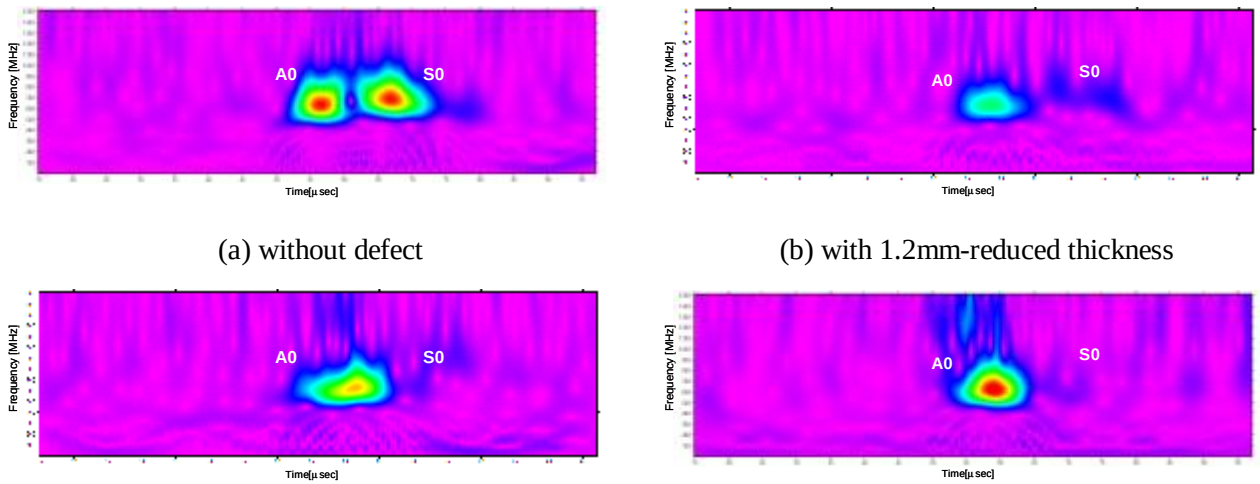

(a) without defect

(b) with 1.2mm-reduced thickness

(c) with 2.4mm-reduced thickness

(d) with 3.6mm-reduced thickness

Figure 8: *Time-frequency analysis of the response with quadrate defect.*

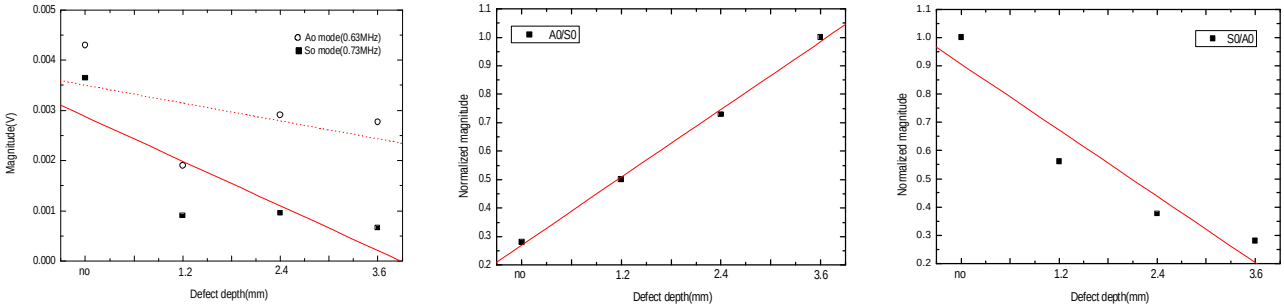

(a) magnitude of A0 and S0 mode versus defect depth

(b) normalized ratio of A0 to S0 mode versus defect depth

(c) normalized ratio of S0 to A0 mode versus defect depth

Figure 9: *Plots of magnitude of A0 and S0 mode and normalized ratio between the magnitudes according to the increment of quadrate defect depth on 6mm thick plate.*

5.2. Elliptical defects of varying depth

Figure 10(a)-(d) show the response received by the air-coupled transducer at the angle of 6.3 degrees after interaction with no defect, 1.2-, 2.4-, and 3.6mm-deep elliptical defect respectively. Similarly to the case of quadrate defect, all signals are dominated by A0 mode. However, the modes in each defect with different depth are attenuated insufficiently than those of quadrate defect. This result indicates that quadrate edge of defect has more influence on the variation of the modes than elliptical one. This fact is represented in Figures 11(a)-(d) which illustrate the results of the time-frequency analysis on the responses with elliptical defect. In these figures, the color of A0 mode which represents the maximum peak amplitude becomes clear and the variation trend of each mode of elliptical defect is similar to that of quadrate defect, excluding the difference of the magnitude. In addition, the magnitude of each mode and its ratio are also varied in a same way as shown in Figures 12(a)-(b). This result shows that the relative variation between A0 and S0 modes could be excellent tool for detecting not only depth of quadrate defect but also that of elliptical defect.

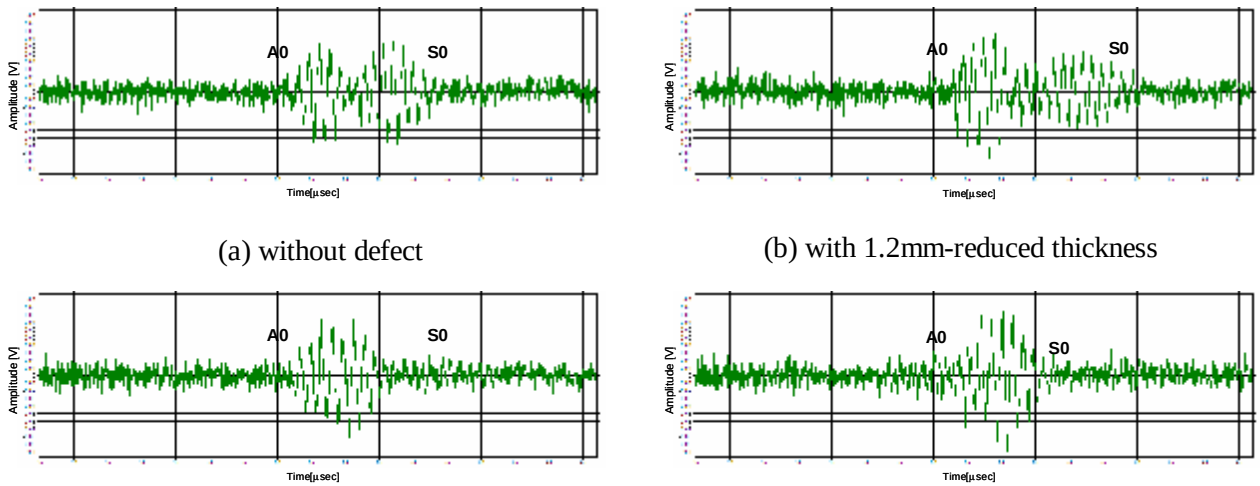

(a) without defect

(b) with 1.2mm-reduced thickness

(c) with 2.4mm-reduced thickness

(d) with 3.6mm-reduced thickness

Figure 10: *Waveforms detected in 6mm thick carbon steel plate with elliptical defect of varying depth, using the receiver with the angle of 6.3degree.*

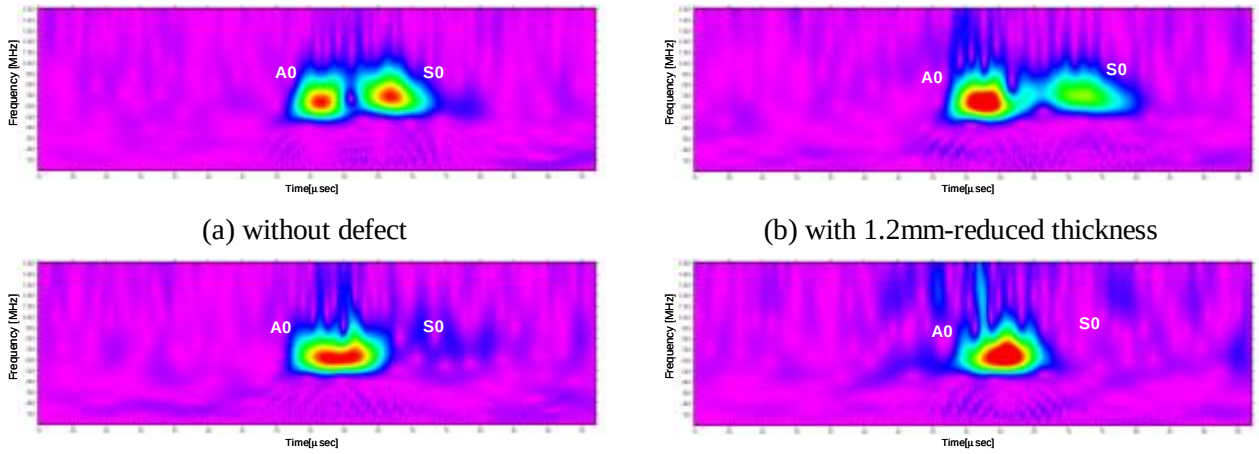

(a) without defect (b) with 1.2mm-reduced thickness

(c) with 2.4mm-reduced thickness (d) with 3.6mm-reduced thickness

Figure 11: *Time-frequency analysis of the responses with elliptical defect.*

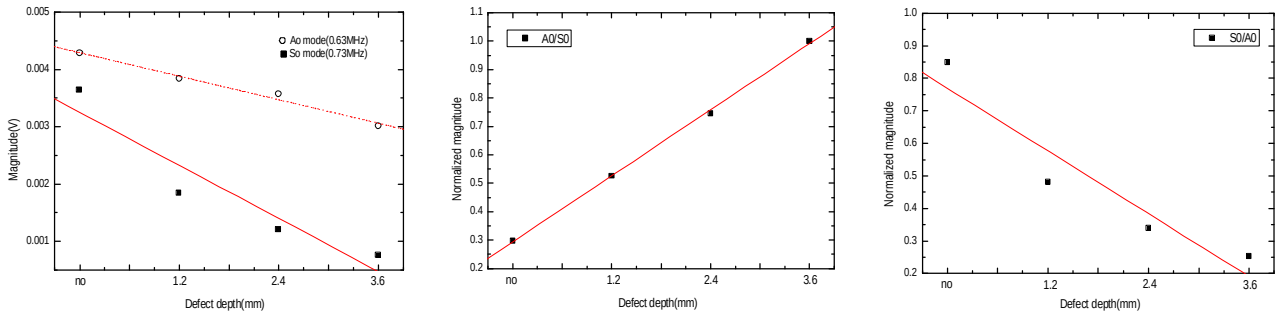

(a) magnitude of A0 and S0 mode versus defect depth

(b) normalized ratio of A0 to S0 mode versus defect depth

(c) normalized ratio of S0 to A0 mode versus defect depth

Figure 12: *Measured frequencies of A0 and S0 modes with elliptical defect on 6mm-thick plate.*

6. Conclusions

The interaction of guided wave mode and the depths of defects with a different shape has been investigated using the measurement on the magnitude of each mode. The result shows that the ratio of magnitude of A0 to that of S0 mode after interaction with defect is proportional to the depth of quadrate defect as well as elliptical one. Therefore, measurement on the ratio of A0 and S0 mode in received signal is useful method for evaluating the defect depth. However, as shown results in this study, such trend of variation of the modes was equally applied to quadrate and elliptical defect. Hence, in order to evaluate the depth and the shape of defect simultaneously, the magnitude of each mode must be considered as well.

7. Acknowledgement

This work was supported by the Ministry of Science & Technology through Basic Atomic Energy Research Institute (BAERI) program.

8. References

[1] Robert E. Green Jr., ``Non-contact Ultrasonic Techniques", *Ultrasonics*, 42:9-16, 2004.

[2] A.S. Murfin and R.J. Dewhurst, ``Estimation of Wall Thinning in Mild Steel Using Laser Ultrasoud Lamb Waves and A Non-steady-state Photo-emf Detector", *Ultrasonics*, 40:777-781, 2002.

[3] D.A. Oursler, J.W. Wagner, ``Narrow-band Hybrid Pulsed Laser/ EMAT System for Noncontact Ultrasonic Inspection Using Angled Shear Waves", *Mater. Eval.*, 53 (5):593–597, 1995.

[4] Francesco Lama di Scalea, Tobias P. Bcrndl, James U. Spicer and B. Boro Djordjevic, ``Remote laser generation of narrow-band surface waves through optical fibers",

IEEE Trans. Ultrason. Ferroelec. Freq. Contr., 46(6):1551-1557, 1999.

[5] A. M. Aindow, R. J. Dewhurst, and S. B. Palmer, ``Laser-generation of directional surface acoustic wave pulses in metals", *Opt. Commun*. 42:116-120, 1982.

[6] D. Clorennec, D. Royer and H. Walaszek, ``Nondestructive Evaluation of Cylindrical Parts Using Laser Ultasonics", *Ultrasonics*, 40:783-789, 2002.

[7] Yijun Shi, Shi-Chang Wooh and Mark Orwat, ``Laser-ultrasonic Generation of Lamb Waves in the Reaction Rorce Range", *Ultrasonics*, 41:623-633, 2003.

[8] C. B. Scruby and L. E. Drain, *Laser ultrasonics: Techniques and applications,* Adam Hilger, Bristol, 1990.

[9] J.L. Rose, , ``A Baseline and Vision of Ultrasonic Guided Wave Inspection Potential", *Transactions of the ASME, Journal of Pressure Vessel Technology*, 124:273-282, 2002.

[10] D.N. Alleyne, and P. Cawley, ``Long Range Propagation of Lamb Waves in Chemical Plant Pipework", *Materials Evaluation*, 55:504-508, 1997.

[11] W.M.D. Wright, D.A. Hutchins, G. Hayward b and Gachagan, ``Ultrasonic Imaging Using Laser Generation and PiezoElectric Air-coupled Detection", *Ultrasonics*, 34:405-409, 1996.

[12] D.A. Hutchins, W.M.D.Wright, G. Hayward, and A. Gachagan, Air-coupled Piezoelectric Detection of Laser-Generated Ultrasound, *IEEE Trans. UFFC,* 41 (6):796–805, 1994.

[13] Kevin C. Baldwin, Tobias P. Berndt and Michael J. Ehrlich, ``Narrowband Laser Generation/Air-coupled Detection: Ultrasonic System for On-line Process Control of Composites", *Ultrasonics*, 37:329-334, 1999.

[14] Daniel Royer, ``Mixed Matrix Formulation for the Analysis of Laser-Generated Acoustic Waves by a Thermoelasitc Line Source", *Ultrasonics*, 39:345-354, 2001.

[15] Hongjoon Kim, Kyongyoung Jhang, Minjea Shin and Jaeyeol Kime, ``A Noncontact NDE Method Using a Laser Generated Focused-Lamb Wave with Enhanced Defect-Detection Ability and Spatial Resolutio", NDT&E International, 39:312-319, 2006.

[16] David N. Alleyne and Peter Cawley, ``The Interaction of Lamb Waves with Defects", *IEEE Trans. Ultrason. Ferroelec. Freq. Contr.*, 39A(3):381-397, 1992.

[17] Kim HM, Lee TH and Jhang KY., ``Non-Contact Guided Wave Technique with Enhanced Mode-Selectivity", *J Korean Soc NDT* , 24(6):597–602, 2004.

[18] David A. Hutchins, William M. D. Wright and Gordon Hayward, ``Air-Coupled Piezoelectric Detection of Laser-Generated Ultrasound", *IEEE Trans. Ultrason. Ferroelec. Freq. Contr.*, 41A(6):796-805, 1994.